Journal of Molecular Catalysis A: Chemical 363–364 (2012) 214–222

Contents lists available at SciVerse ScienceDirect

Journal of Molecular Catalysis A: Chemical

journal homepage: www.elsevier.com/locate/molcata

Further insight in the minor/major concept using hydrogen pressure effect in asymmetric hydrogenation

A. Aloui [a,b], F. Delbecq [b], P. Sautet [b], C. De Bellefon [a,*]

[a] University of Lyon, CPE Lyon, CNRS, Laboratoire de Génie des Procédés Catalytiques, UMR 5285, 43, bd du 11 novembre 1918, 69616 Villeurbanne Cedex, France
[b] University of Lyon, ENS Lyon, CNRS, Laboratoire de Chimie, UMR 5182, Ecole normale supérieure de Lyon, 15 parvis René Descartes, 69342 Lyon Cedex 07, France

ARTICLE INFO

Article history:
Received 27 February 2012
Received in revised form 11 June 2012
Accepted 16 June 2012
Available online 7 July 2012

Key words:
Asymmetric hydrogenation
Hydrogen pressure
Enantiomeric excess
(R,R)-Me-BPE
M-acrylate
E-emap

ABSTRACT

The catalytic system prepared from $[Rh(COD)_2]BF_4$ and (R,R)-Me-BPE provides a spectacular detrimental hydrogen pressure effect on ee from 94% down to 56% in the hydrogenation of methylacrylate, whereas it has a strong beneficial effect on the hydrogenation of E-emap (from 42% up to 72%). The kinetic parameters have been determined for both systems and have helped to identify the most enantioselective controlling steps (MECS). Accordingly, further explanations for the structure-ee and hydrogen pressure relationship are proposed.

1. Introduction

Catalytic enantioselective hydrogenation is one of the most promising and industrially viable methodologies for the synthesis of chiral α/β dehydroamino acids and their derivates which are of key importance to the pharmaceutical, flavour and fragrance, animal health, agrochemical and functional materials industries [1–5]. Numerous efforts were spent to reach high enantioselectivity through the synthesis of different families of chiral ligands thus calling for high throughput methods for the screening (HTS) of the very large chemical diversity available over four work decades [6–9]. Despite a large number of researchers focused on asymmetric hydrogenation, there are no predictive tools to design a catalytic system for a given substrate. This is as yet due to the still unclear relation between the molecular properties (steric and electronic factors) of the catalyst/substrate system and macroscopic factors (concentrations, pressure, temperature) influencing the enantioselectivity. Thus, the origin of enantioselectivity remains uncertain and still motivates much ongoing research [10–18]. While screening methods are the only way to select enantioselective catalysts, only mechanistic and kinetic studies can help to bring a fundamental understanding of enantio-discriminating factors.

Rhodium complexes are often used as catalysts for the enantioselective hydrogenation reactions. Two mechanisms are proposed (Scheme 1). The unsaturated mechanism, proposed very early by Brown and Halpern, is strongly supported by kinetic measurements, NMR characterization of reactive intermediates and X-ray analyses [10–14,19–26]. In this mechanism, diastereomeric complexes are formed by coordination of a prochiral substituted olefin to the chiral catalyst-solvent complex through the C=C bond and the oxygen atom of the pendant amide group. These intermediates react in a sequence of elementary steps (oxidative addition of hydrogen, insertion and reductive elimination to give enantiomer products). Recent results have provided considerable refinement of the enantioselective hydrogenation mechanism. The dihydride mechanism is an alternative with the hydrogen oxidative addition step occurring before the substrate coordination step [27–31].

Like any reaction with selectivity issues due to a multiple reaction network, enantioselective reactions are influenced by many macroscopic parameters among which the hydrogen pressure, i.e. the actual hydrogen concentration, is significant. As early as the 1970s, several studies have reported the effect of hydrogen pressure on enantioselectivity [15–18]. In a recent paper, using a large number of catalytic systems, it has also been demonstrated that the hydrogen pressure effect on ee is rather general and that an equivalent distribution between beneficial and detrimental pressure effects on enantioselectivity prevails [32]. Some quantitative explanations for the hydrogen pressure-enantioselectivity dependence are given in the literature but plausible reasons are not yet

* Corresponding author. Tel.: +33 472 43 17 54; fax: +33 472 43 16 73.
E-mail address: claude.debellefon@lgpc.cpe.fr (C. De Bellefon).

1381-1169/$ – see front matter © 2012 Elsevier B.V. All rights reserved.
http://dx.doi.org/10.1016/j.molcata.2012.06.012

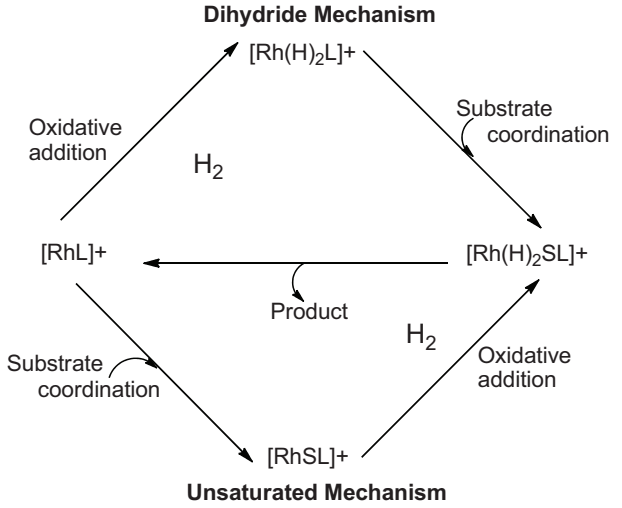

Scheme 1. Mechanisms of Rh(I)-catalysed hydrogenation. L is a bidentate chiral diphosphine. S is a bidentate substrate.

known. The understanding of this relationship is still one of the most challenging questions in the field of asymmetric catalysis. Further, the mechanism of rhodium-catalysed hydrogenation of enamides, as discussed in previous paper [33], strongly depends on the electronics of the substrate, particularly the ability to stabilize the forming negative charge in the dihydride intermediates at either the α or the β carbon of the olefin double bond. This dependence can have a significant impact on the origins of enantioselectivity.

The present study was therefore undertaken to provide some further understanding of these issues. In fact, this work will focus on the impact of substrate structure and hydrogen pressure on ee. The chosen reaction is the hydrogenation of acetamidoacrylates with rhodium complexes. The followed methodology is the choice of the reaction mechanism, the quantification of the kinetic constants involved in the elementary steps, the identification of the most enantioselective controlling steps and the proposal of a structure-enantioselectivity relationship.

2. Experimental

2.1. Chemicals and analysis

The catalyst precursor $[Rh(COD)_2]^+$ BF_4^- (Alfa-Aesar) and the ligand (R,R)-Me-BPE (Strem) were used as received. Methanol was degassed and purged under argon prior to use. A ligand/Rh ratio of 1.05 was used. The catalyst was prepared ex situ from $[Rh(COD)_2]^+$ BF_4^- and the (R,R)-Me-BPE in methanol. This mixture was stirred at room temperature for about 1/2 h and stored at 6 °C at which temperature the catalyst was stable as proved by reproducible catalytic tests. M-acrylate (methyl 2-acetamidoacrylate) was provided from Aldrich whereas E-emap (ethyl 4-methyl-3-acetamido-2-pentanoate) and MAC (methyl Z-α-acetamido-cinnamate) were prepared according to the published procedure [34,35]. Conversions yields and enantioselectivities were determined by gas chromatographic analysis on a Lipodex E (10 m × 0.1 mm) and CHIRASILVAL (25 m × 0.25 mm) column. Experimental enantiomeric excess is obtained as: ee = ([R] − [S])/([R]+[S]).

2.2. Reactors and chemical regime

Hydrogenation experiments were performed in a stainless steel mini-autoclave of 15 cm^3 equipped with a magnetic stirrer (2200 rpm, k_La up to 0.87 s^{-1}), under hydrogen pressure (2–41 bar) in degassed MeOH (4 cm^3). Samples were periodically collected and analysed by GC. The reaction regime under which the rate data were obtained was kinetically controlled. The effects of catalyst loading and the stirring rate on the apparent rate of reaction were investigated. The initial rate of reaction was found to increase linearly with catalyst charge (from 10^{-5} to 10^{-4} kmol m^{-3} of catalyst), also, it is independent of agitation speed beyond 2200 rpm. This indicated that external mass-transfer resistance is not significant under the operating conditions. With the help of our experimental measures, we extrapolated the correlation for solubility of hydrogen in methanol described by Liu [36,37] by according to the range of operating conditions (hydrogen pressure and temperature).

Table 1
Range of conditions used in the kinetic study.

Conditions	Operating range	
	M-acrylate	E-emap
[Substrate], kmol m^{-3}	0.02–0.3	0.025–0.14
PH_2, bar	2–41	1.3–41
H_2, kmol m^{-3}	0.0084–0.14	0.0084–0.14
Rh, kmol m^{-3}	10^{-4}	10^{-3}

2.3. Range of operating conditions

The different operating conditions used in the kinetic study for the selected catalytic systems are summarized in Table 1. All experiments were performed at 308 K.

3. Results and discussion

3.1. Choice of the catalytic system

Understanding structure-enantioselectivity relationship requires working on systems, i.e. catalyst + chiral diphosphine + substrates, presenting very strong hydrogen pressure effects for a very small change in the substrate structure. This would ensure a quantitative and high quality for the kinetic parameters estimation and a straightforward attribution of the effect of the substrate changes. Thus, a catalytic system with opposite hydrogen pressure effect on ee would be the best case. Three substrates, methyl Z-α-acetamidocinamate (MAC), methyl 2-acetamidoacrylate (M-acrylate), and ethyl 4-methyl-3-acetamido-2-propanoate (E-emap) were selected. They are all readily available in large quantities and have been the subject of a large number of publications. These substrates present stepwise changes in their structure such as the position of the acetamido group, the steric hindrance and the substituent nature at the sp^2 carbons (Scheme 2).

The choice of the catalyst was operated by screening a restricted library of 6 commercially available chiral diphosphines (Scheme 3) over a large range of hydrogen pressure (2–41 bar) for the three different substrates (MAC, M-acrylate and E-emap) and at 308 K (Table 3). The choice of these 6 chiral diphosphines was motivated by their known ability to lead to higher ee, and so to induce hydrogen pressure effect, compared to other chiral diphosphines that are not prone to hydrogen effect such as the BINAP's [32].

In order to verify our methodology, a first series of experiments was performed and the ee was compared to published results (Table 2). It appears that under the tested conditions and for the selected couples substrate/ligand, similar ee are obtained, except in the case of (R,R)-Me-BPE for which the ee variation with the pressure is more significant.

Then, the selected reaction systems were evaluated. The results show a very small hydrogen pressure effect for MAC whereas in pioneering works, a larger effect has been observed with this substrate

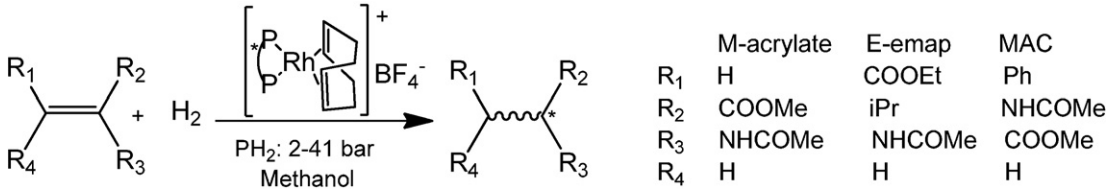

Scheme 2.

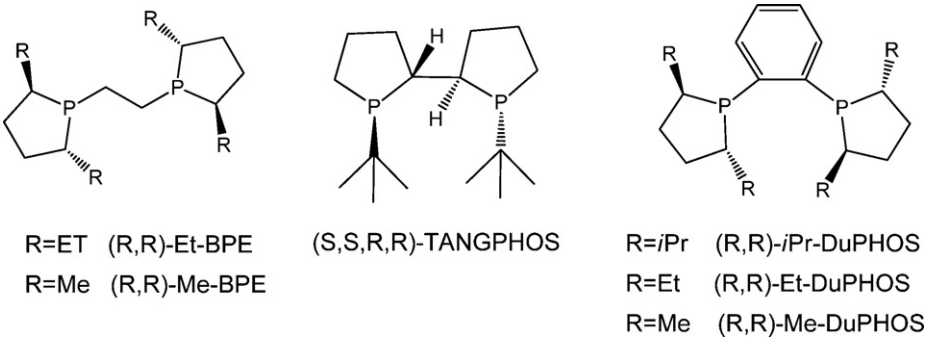

Scheme 3. Chiral diphosphines used in this work.

Table 2
Comparison of ee obtained in this work with literature data under similar operating conditions.

Diphosphine	Substrate	PH_2	ee	Ref.
(R,R)-Et-BPE	MAC	2	77	This work
		5	79	[32]
(R,R)-Me-BPE	MAC	41	80	This work
		30	76	[32]
	E-emap	41	−72	This work
		30	−62	[32]
(S,S,R,R)-TANGPHOS	MAC	2	99	This work
		5	98	[32]
		1.4	99	[38]*
	E-emap	41	32	This work
		30	32	[32]
(R,R)-*i*Pr-DuPHOS	MAC	2	95	This work
		5	96	[32]

Conditions: MeOH, [Rh]/[L] = 1.05, 308 K; (*): 298 K, [Rh]/[L] not available

with the DIPAMP chiral diphosphine [13]. However, an interesting system involving the Me-BPE chiral diphosphine, presents two opposite effects with hydrogen pressure depending on the substrate: a beneficial effect with M-acrylate ($\Delta ee = -38\%$) and a detrimental effect with E-emap ($\Delta ee = +30\%$) (Table 3). These two systems were thus investigated by detailed kinetic studies.

Conditions: MeOH; L/Rh = 1.05; 308 K; ee (%) = ([R] − [S])/([R] + [S]); ee_2 (%) = ee at 2 bar hydrogen pressure; ee_{41} (%) = ee at 41 bar hydrogen pressure. $\Delta ee = |ee_{41}| - |ee_2|$%. All results are at close to quantitative conversion. For the sake of conciseness, only ee values at boundaries (2 and 41 bar) of the hydrogen pressure range are presented. Further data can be found in the supplementary material. n.a.: not tested.

Table 3
Results of the variation of ee upon hydrogen pressure from 2 to 41 bar.

Catalyst (Rh/L)	MAC			M-acrylate			E-emap		
L=	ee_2	ee_{41}	Δee	ee_2	ee_{41}	Δee	ee_2	ee_{41}	Δee
(R,R)-Et-BPE	77	70	−7	79	77	−2	n.a.	n.a.	n.a.
(R,R)-Me-BPE	89	80	−9	94	56	−38	−42	−72	+30
(S,S,R,R)-TANGPHOS	99	98	−1	98	95	−3	90	32	−58
(R,R)-*i*Pr-DuPHOS	95	98	3	58	30	−20	n.a.	n.a.	n.a.
(R,R)-Et-DuPHOS	27	24	−3	2	1	−1	n.a.	n.a.	n.a.
(R,R)-Me-DuPHOS	n.a.	n.a.	n.a.	96	91	−5	+97	96	−1

3.2. Kinetic study

A quantitative kinetic study for the hydrogenation reaction was undertaken on the two catalytic systems identified previously. The influence of reaction parameters such as substrate concentration and hydrogen pressure has been evaluated.

3.2.1. M-acrylate (methyl-2-acetamidoacrylate)

The typical concentration vs. time profiles of M-acrylate and the two enantiomeric products is given in Fig. 1a. Enantiomer R is the main reaction product within the range of hydrogen pressure investigated here.

The initial rate of formation of isomer S, at constant hydrogen pressure (6 bar), does not vary with the substrate concentration, ranging from 0.02 to 0.3 kmol m^{-3} (Fig. 1b). That of isomer R increases slowly at low concentration and then reaches a plateau. Overall and despite the rate increase of isomer R, the enantiomeric excess does not vary much with the substrate concentration with an average value of 85 ± 5% (see supplementary material). Therefore, the concentration of the substrate does not much affect the enantioselectivity. The effect of the hydrogen pressure was also tested. A significant increase of the initial rate with pressure has been noted, which seems to level off for the major R enantiomer. Thus the rate of formation of the minor S enantiomer is proportionally increased with the increase of hydrogen pressure (Fig. 2a). As a consequence, a detrimental effect of hydrogen pressure on enantioselectivity is observed, and the enantiomeric excess decreases from 94 to 56% with increasing the hydrogen concentration in the liquid phase (Fig. 2b).

3.2.2. E-emap (ethyl-4-methyl-3-acetamido-2-propanoate)

In contrast to M-acrylate, the major product is the S enantiomer. As seen above for M-acrylate, different hydrogenation tests were also undertaken with E-emap at different operating conditions. The linear dependence of the initial rate on substrate concentration suggests that the formation of the enantiomers was of first order with respect to E-emap (Fig. 3a). However, since the rate

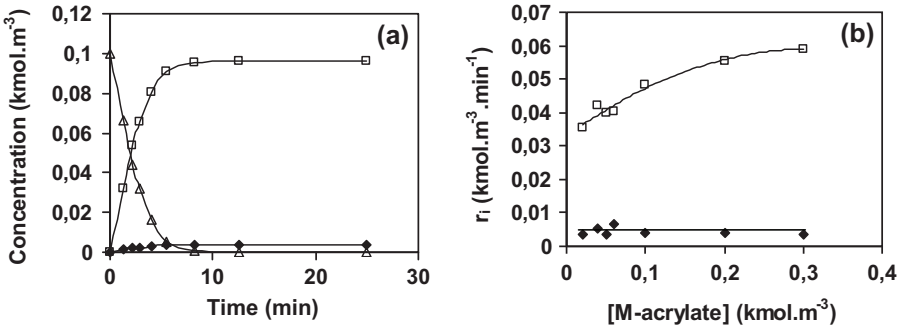

Fig. 1. (a) Concentration vs. time profiles for the hydrogenation of M-acrylate; (△) [M-acrylate]; (□) [R]; (♦) [S] ([M-acrylate] = 0.1 kmol m^{-3}; [Rh] = 10^{-4} kmol m^{-3}; L/Rh = 1.05; PH_2 = 2 bar; T = 308 K) and (b) dependence of the observed initials rates r_{iR} (□) and r_{iS} (♦) on substrate concentration ([Rh] = 10^{-4} kmol m^{-3}; L/Rh = 1.05; PH_2 = 6 bar; T = 308 K). The lines are included to show the profiles clearly and do not represent a model.

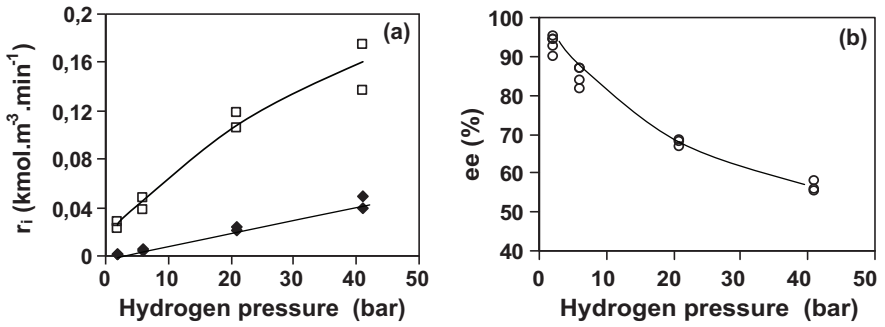

Fig. 2. (a) Dependence of the observed initials rates r_{iR} (□) and r_{iS} (♦) on hydrogen pressure and (b) dependence of the enantiomeric excess on hydrogen pressure ([M-acrylate] = 0.1 kmol m^{-3}; [Rh] = 10^{-4} kmol m^{-3}; L/Rh = 1.05; T = 308 K). The lines are included to show the profiles clearly and do not represent a model.

dependence on the substrate concentration is similar for both enantiomers, no effect is observed on the enantiomeric excess (Fig. 3b).

Increasing the hydrogen pressure affords a noticeable increase in enantioselectivity, |ee| varying from 20 to 70% over a broad pressure range of 40 bar (Fig. 4b).

3.3. Kinetic modelling

As mentioned in the introduction, two mechanisms can be considered for asymmetric hydrogenations involving a chiral diphosphine rhodium complex (Scheme 1). The dihydride mechanism depicts the formation of two rhodium hydrides diastereomers from the chiral Rh-diphospine solvated complex (I) followed by coordination of the substrate A (Scheme 4). It has been demonstrated that these two isomers are rapidly exchanged without complete dissociation of hydrogen [27]. Thus, this step can be described by a simple equilibrium (Eq. (1)). Hence, any hydrogen pressure effect on ee is related to the interplay between steps 1, 2 and 3 as long as the rate determining steps are taking place after substrate coordination. Under these considerations, the possibility

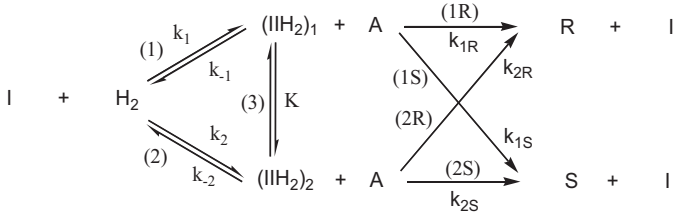

Scheme 4. Elementary steps for the dihydride mechanism of Rh(I)-catalysed asymmetric hydrogenations.

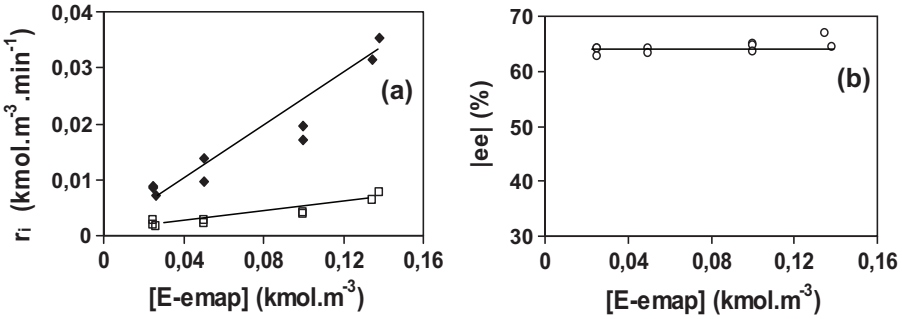

Fig. 3. (a) Dependence of the observed initials rates r_{iR} (□) and r_{iS} (♦) on substrate concentration ([Rh] = 10^{-3} kmol m^{-3}; L/Rh = 1.05; T = 308 K; PH_2 = 6 bar) and (b) dependence of the enantiomeric excess on conversion of E-emap ([E-emap] = 0.1 kmol m^{-3}; [Rh] = 10^{-3} kmol m^{-3}; L/Rh = 1.05; T = 308 K; PH_2 = 2 bar). The lines are included to show the profiles clearly and do not represent a model.

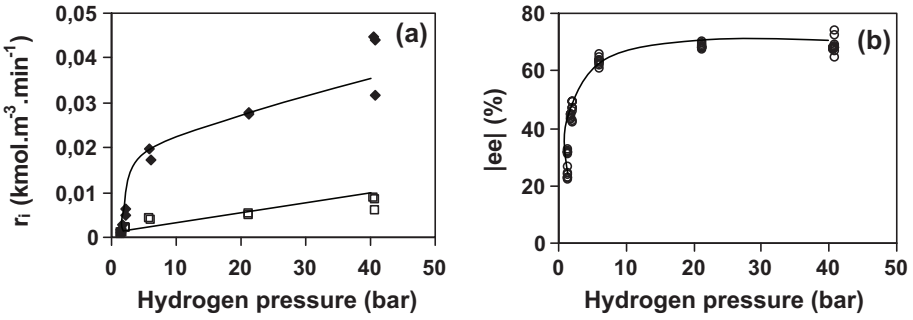

Fig. 4. (a) Dependence of the observed initials rates r_{iR} (□) and r_{iS} (♦) on hydrogen pressure and (b) dependence of enantiomeric excess on hydrogen pressure ([E-emap] = 0.1 kmol m^{-3}; [Rh] = 10^{-3} kmol m^{-3}; L/Rh = 1.05; T = 308 K). The lines are included to show the profiles clearly and do not represent a model.

of hydrogen pressure effect on ee within the dihydride mechanism can be discussed.

$$K = \frac{[(IIH_2)_1]}{[(IIH_2)_2]} \quad (1)$$

$$[Rh]_{tot} = [I] + [(IIH_2)_1] + [(IIH_2)_2] \quad (2)$$

Taking into account the equilibrium (Eq. (1)), the rhodium mass balance (Eq. (2)) and considering the steady-state approximation on the rhodium solvated complex (I), the product formation rate can be deduced (Eq. (3)).

$$r_R = (Kk_{1R} + k_{2R})[A]\frac{K\,B\,[Rh]_{tot}}{1 + B + BK} \quad \text{with :} \quad B = \frac{k_1 + k_2}{Kk_{-1} + k_{-2}}[H_2] \quad (3)$$

$$\frac{r_R}{r_S} = \frac{Kk_{1R} + k_{2R}}{Kk_{1S} + k_{2S}} \quad (4)$$

The rate for reaction (S) is obtained by switching the R and the S indices. As the instantaneous enantioselectivity ratio is related to the ratio of the rate of formation of the R and the S enantiomers (Eq. (4)), it demonstrates that ee cannot vary with the hydrogen pressure. Indeed, all attempts to fit this model to the experimental data failed. Note however that if the equilibrium of reaction (3) would have been hydrogen dependent, this conclusion would not hold. Another reason for rejection of the dihydride mechanism lies in the fact that the operating conditions under which the diastereomers of rhodium dihydrides have been observed are far from those being applied in our work [30]. Hence, for the catalytic systems studied in this work, the kinetic model derived from the dihydride mechanism can be disregarded.

On the contrary, the hydrogen pressure enantioselectivity dependence has been proved for MAC hydrogenation with [Rh(R,R)-DIPAMP] complex proceeding through the unsaturated mechanism [13]. Many examples have been also found in the literature [32]. The simplified unsaturated mechanism presents six elementary steps (Scheme 5).

The application of the steady-state approximation on diastereomers intermediates leads to the following rate laws (Eq. (5)).

$$r_R = \frac{k_{1R}k_{2R}}{(k_{-1R} + k_{2R}[H_2])} \frac{[A][Rh]_{tot}[H_2]}{\left(1 + (k_{1R}[A]/k_{-1R} + k_{2R}[H_2]) + (k_{1S}[A]/k_{-1S} + k_{2S}[H_2])\right)} \quad (5)$$

$$\frac{r_R}{r_S} = \frac{k_{1R}k_{2R}(k_{-1S} + k_{2S}[H_2])}{k_{1S}k_{2S}(k_{-1R} + k_{2R}[H_2])} \quad (6)$$

The rate for reaction (S) is obtained by switching the R and the S indices. Thus for the unsaturated mechanism, the possible pressure effect of hydrogen on ee is clearly evidenced (Eq. (6)). The model derived from the unsaturated mechanism will be the subject of this modelling section.

The estimation of the unknown model parameters is performed through the entire concentration vs. time profiles by means of React'Op software (ChemInform-St. Petersburg) [39]. For the M-acrylate hydrogenation, Fig. 5 illustrates the experimental and calculated data, which suggests that the kinetic model provides satisfactory agreement between them. For clarity, only a few experiments are represented in Fig. 5a; the lines represent the model and points are experimental results.

The results of the estimation with global kinetics indicate that only 5 kinetic constants on a set of 6 can be identified, 4 being true mechanistic constants (k_{1R}; k_{-1R}; k_{2R}; k_{2S}), and the other one being a ratio of two mechanistic constants ($K_S = k_{1S}/k_{-1S}$). Thus k_{1S} and k_{-1S} are strongly correlated and not distinguishable. The correlation matrix is given in the supplementary information.

Table 4 summarizes numerical values of the estimated kinetic constants. The parameters which are responsible for the description of the rate for the main product formation were determined with a satisfactory accuracy. In order to adapt the kinetic model to experimental results, the relation $k_{-1S} \gg k_{2S}$[H2] has been supposed, and its validity has been checked by a numerical estimation. Hence the rate laws corresponding to the catalytic cycle of enantiomer S can be simplified:

$$r_S = K_S k_{2S}\left(\frac{[A][H_2][Rh]}{1 + (k_{1R}[A]/k_{-1R} + k_{2R}[H_2]) + K_S[A]}\right) \quad \text{with :} \quad K_S = \frac{k_{1S}}{k_{-1S}} \quad (7)$$

All attempts to determine the equilibrium of reaction 1R and 1S (Scheme 5) by tracing intermediates using ^{31}P NMR failed despite

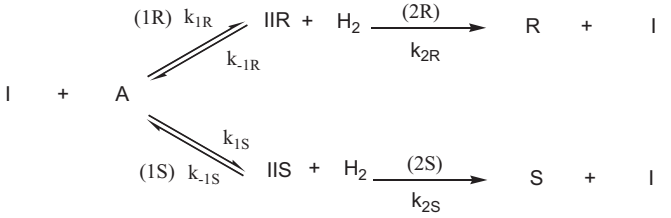

Scheme 5. Elementary steps for unsaturated mechanism of Rh(I)-catalysed asymmetric hydrogenation.

Table 4
Estimated kinetic parameters for M-acrylate hydrogenation.

Kinetic parameter	Unit	Estimated value
k_{1R}	m^3 kmol^{-1} min^{-1}	$(1.3 \pm 0.6) \times 10^5$
k_{-1R}	min^{-1}	$(3.2 \pm 0.9) \times 10^2$
k_{2R}	m^3 kmol^{-1} min^{-1}	$(2.6 \pm 0.2) \times 10^4$
k_{2S}	m^3 kmol^{-1} min^{-1}	$(1.4 \pm 0.8) \times 10^4$
$K_S = k_{1S}/k_{-1S}$	m^3 kmol^{-1}	16.6 ± 3

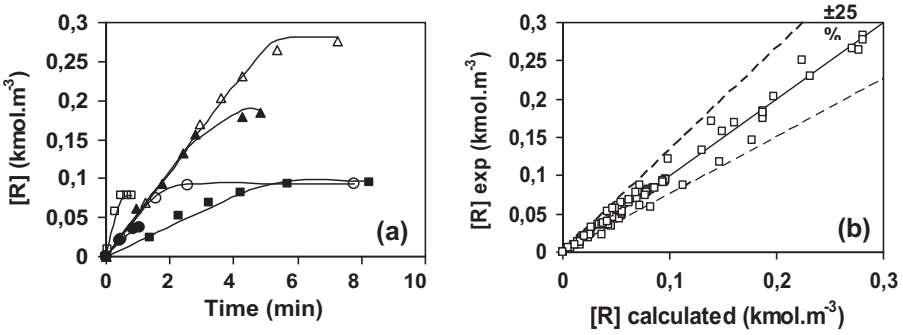

Fig. 5. (a) Concentration vs. time profiles. Comparison between experimental data (symbols) and model (lines); Conditions (■) [M-acrylate] = 0.1 kmol m^{-3} PH_2 = 2 bar; (□) [M-acrylate] = 0.1 kmol m^{-3} PH_2 = 41 bar; (●) [M-acrylate] = 0.04 kmol m^{-3} PH_2 = 6 bar; (○) [M-acrylate] = 0.1 kmol m^{-3} PH_2 = 6 bar; (▲) [M-acrylate] = 0.2 kmol m^{-3} PH_2 = 6 bar; (△) [M-acrylate] = 0.3 kmol m^{-3} PH_2 = 6 bar and (b) calculated vs. experimental concentration for R (the same results have been obtained with S and M-acrylate).

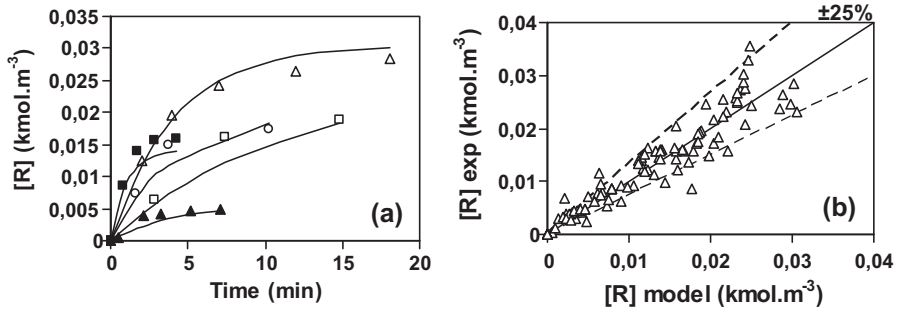

Fig. 6. (a) Concentration vs. time profiles. Comparison between experimental data (symbols) and model (lines); conditions: (■) [E-emap] = 0.1 kmol m^{-3}, PH_2 = 41 bar; (□) [E-emap] = 0.1 kmol m^{-3}, PH_2 = 2 bar; (○) [E-emap] = 0.1 kmol m^{-3}, PH_2 = 6 bar; (▲) [E-emap] = 0.025 kmol m^{-3}, PH_2 = 6 bar; (△) [M-acrylate] = 0.14 kmol m^{-3}, PH_2 = 6 bar and (b) calculated vs. experimental concentration for R (the same results have been obtained with S and E-emap).

the different applied methods for mixture preparation, and only a few secondary species have been identified.

The estimation of the kinetic parameters for the second system was also performed by React'Op, using the kinetic model derived from the unsaturated mechanism as explained above. The kinetic model fits the experimental data well (Fig. 6), but the estimation allows only the identification of 4 parameters due to the strong correlation between pairs of rate constant (k_{-1R}, k_{2R}) and (k_{-1S}, k_{2S}) corresponding to substrate decoordination and oxidative addition steps (Table 5).

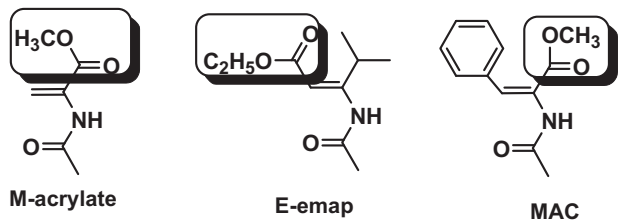

Scheme 6.

Table 5
Estimated kinetic parameters for E-emap hydrogenation.

Kinetic parameters	Unit	Estimated value
k_{1R}	m^3 kmol^{-1} min^{-1}	$(2.2 \pm 0.7) \times 10^2$
k_{1S}	m^3 kmol^{-1} min^{-1}	$(3.5 \pm 2) \times 10^3$
$K = (k_{-1R}/k_{2R})$	m^3 kmol^{-1}	0.076 ± 0.003
$K' = (k_{-1S}/k_{2S})$	m^3 kmol^{-1}	0.435 ± 0.2

The experimental work has demonstrated that the rate formation of enantiomers was of first order with respect to the E-emap concentration, so the kinetic model can be written as follows:

$$r_R = \frac{k_{1R}([A][H_2][Rh])}{K + [H_2]} \quad (8)$$

$$r_S = \frac{k_{1S}([A][H_2][Rh])}{K' + [H_2]} \quad (9)$$

This implies:

$$\frac{k_{1R}[A]}{k_{-1R} + k_{2R}[H_2]} \ll 1 \quad \text{and} \quad (10)$$

$$\frac{k_{1S}[A]}{k_{-1S} + k_{2S}[H_2]} \ll 1 \quad (11)$$

By using the estimated kinetic parameters of each system, it has been possible to reproduce the experimental results; in fact the model predicts the enantiomeric excess and hydrogen pressure dependence, which validates again our estimate (Fig. 7).

The kinetic modelling with E-emap and M-acrylate did not provide full set of kinetic constants separate due to the strong correlation between some constants. Hence, considering the ratio between the kinetic constants of enantiomeric elementary steps lies in the range $0.002 \leq k_{iR}/k_{iS}$ or $k_{iS}/k_{iR} \leq 500$ [40], the evaluation of rate constant corresponding to the M-acrylate is achievable. In fact, the lowest value for k_{-1S} (6.10^4 min$^{-1} \leq k_{-1S}$) is estimated since the ratio K_S is no longer constant and the numerical estimation leads to divergence. However, the upper limit of k_{-1S} is imposed by that relation $0.002 \leq k_{-1S}/k_{-1R} \leq 500$, and that maximum value of k_{-1S} is 1.57×10^5 min^{-1}. The upper and lower values of k_{-1S} are considered thereafter (Table 6). For E-emap, the rate constant still not evaluated separately.

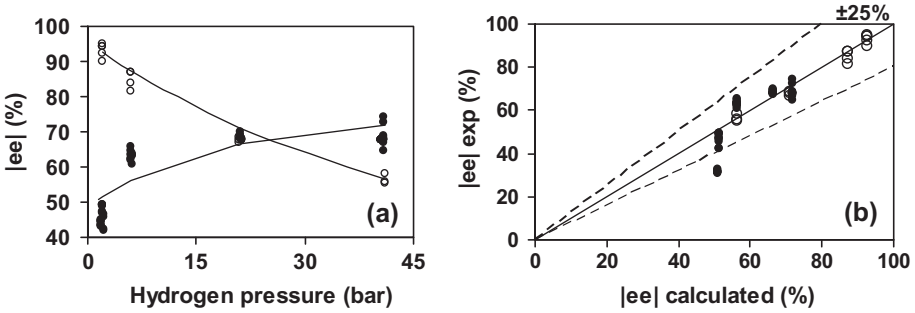

Fig. 7. (a) Dependence of |ee| on hydrogen pressure; comparison between experimental data and model. The lines correspond to the model and (b) calculated vs. experimental |ee|; (●) E-emap; (○) M-acrylate.

The ratio between the kinetic constants of enantiomeric elementary steps (k_{iR}/k_{iS} or k_{iS}/k_{iR} with i the step number) has been investigated to understand the structure-enantioselectivity and hydrogen pressure relationship, and thus the identification of the most enantioselective controlling steps (Table 6). That calculation was carried out for M-acrylate/(R,R)-Me-BPE and MAC/(R,R)-DIPAMP [13]. This last was the only system for which the kinetic parameters have been identified [41].

At first sight, it is clear that all the elementary steps are involved in the enantioselection process, i.e. $k_{iR}/k_{iS} \neq 1$. For M-acrylate, the coordination and the decoordination of the substrate are heavily controlling for the enantioselection process, whereas for MAC, the oxidative addition of hydrogen is the dominating step.

The explanation of the shift of the most enantioselective controlling steps may be found in the structure of the substrates (Scheme 6). In the case of M-acrylate, the olefin double bond is electron poor compared to that of MAC which has an electron-donor substituent. This makes the relative electronic density on the two olefin carbon atoms different. E-emap is supposed to present a similar electronic density to that of MAC, owing to the presence of two substituents on the olefin carbon atoms with opposite inductive effect. Hence, the same enantiomeric determining step, i.e. the oxidative addition as it plays for the enantioselective hydrogenation of MAC, is foreseen for E-emap. Nevertheless, we are not able to further support this assumption since the values of the kinetic parameters cannot be determined as discussed previously. According to previous experimental [42] and computational [33,43] works, for α-dehydroamino substrates such as MAC and M-acrylate, the reaction mechanism should proceed through α-monohydride pathway, and for the β-dehyroamino substrates, such as E-emap, through β-monohydride pathway. Indeed, albeit it may be that the hydride transfer step (migratory insertion) is the same for MAC and for M-acrylate, the most enantioselective controlling step is different and can be driven by other factors such as the electronic density or steric properties at the double bond. Further, α and β-monohydride pathways lead to opposite enantioselectivity, but it can not explain the hydrogen pressure effect. Even if we fully agree that opposite enantioselectivity may be obtained for one of the enantioselective controlling steps (that of migratory insertion), it remains that the global measured enantioselectivity relies on many interplaying steps.

Concerning the effect of hydrogen pressure, a previous report has shown that, considering the unsaturated mechanism, the enantiomeric excess dependence with hydrogen pressure is related to the sign of the derivative of ee with hydrogen pressure (Eq. (12)) [32].

$$\mathrm{Sign}\frac{\mathrm{dee}}{\mathrm{d}[\mathrm{H_2}]_\mathrm{L}} = \mathrm{Sign}\frac{\mathrm{dee}}{\mathrm{dPH_2}} = \mathrm{Sign}\Delta\mathrm{ee} = \mathrm{Sign}(\alpha);\ \alpha = \left(\frac{k_{-1\mathrm{R}}}{k_{2\mathrm{R}}} - \frac{k_{-1\mathrm{S}}}{k_{2\mathrm{S}}}\right) \quad (12)$$

In which, △ee is the difference between the ee measured at higher pressure and the ee measured at lower pressure. In practice, four situations can be encountered. For catalytic systems providing R configurations (ee > 0), the hydrogen pressure effect can be beneficial (Δee > 0) or detrimental (Δee < 0). Conversely, for S configurations (ee < 0), the hydrogen pressure effect can be beneficial (Δee < 0) or detrimental (Δee > 0). For the two substrates E-emap and M-acrylate, △ee values amount −30 and −38 with configurations S and R respectively. Thus, a beneficial hydrogen pressure effect for E-map is observed and a detrimental impact plays for M-acrylate. This experimental observation is perfectly in line with the sign of the △ parameter for E-emap ($\alpha < 0$) and M-acrylate ($\alpha < 0$). More generally, the values of kinetic constants of independent steps determined by e.g. NMR or computational methods may be used to compute the sign of α hence to predict the effect of hydrogen pressure on ee.

Another facet of asymmetric homogeneous catalysis is the major/minor concept, i.e. the minor diastereomer leads to the major product of the reaction, contrary to the lock-and-key concept derived for enzyme catalysis. The lock-and-key and major/minor concepts are two over-simplified forms of the mechanism of catalytic asymmetric hydrogenation and were often taken as rivals and exclusive. Heller and co-workers proposed the idea of a possible coexistence of the two concepts through an intellectual exercise based on the set of the kinetic constants identified experimentally by Halpern for MAC/(R,R)-DIPAMP system [44]. Permutation of the 6 rate constants leads to cases for which the concentrations of both diastereomers could be reversed with

Table 6
Ratios of elementary steps constants.

System		$i=1$ substrate coordination	$i=-1$ substrate decoordination	$i=2$ oxydative addition of H_2	ee at 1 bar (R or S)
k_{iR}/k_{iS}	M-acrylate (R,R)-Me-BPE	**234**	**190**	1.85	94 (R)
or		**156**	**500**	1.85	
k_{iS}/k_{iR}	MAC (R,R)DIPAMP	1.9	18	**500**	97 (R)

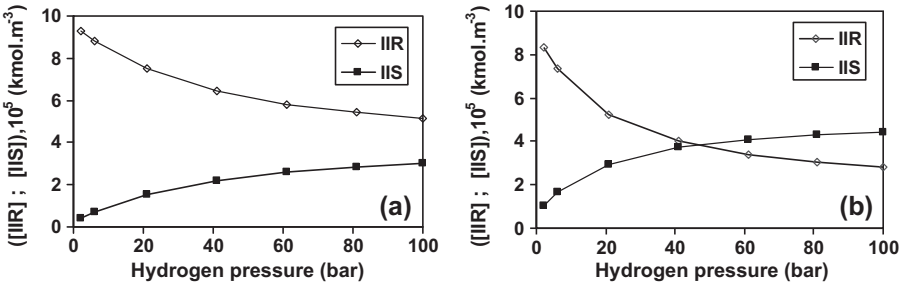

Fig. 8. Diastereomeric concentration vs hydrogen pressure ([M-acrylate] = 0.1 kmol m^{-3}, [Rh] = 10^{-4} kmol m^{-3}) (a) $k_{1R} = 1.9 \times 10^5$ m^3 kmol^{-1} min^{-1}, (b) $k_{1R} = 0.7 \times 10^5$ m^3 kmol^{-1} min^{-1}.

the hydrogen pressure, i.e. going from the major/minor description to the lock-and-key. The obtained results for M-acrylate can contribute to this discussion. In fact, considering the range of respective confidence interval, the value impact of each rate constant on the concentration of both diastereomers has been studied. Asymptotic profiles without crossing for the diastereomeric concentration, i.e. with the lock-and-key concept operating, were obtained except for some values of k_{1R}. Within the confidence interval $[0.7 \times 10^5;\ 1.9 \times 10^5]$, for $k_{1R} > 1.1 \times 10^5$ kmol m^{-3}, an asymptotic behaviour with no crossing is observed (Fig. 8a) whereas values of $k_{1R} \leq 1.1 \times 10^5$ kmol m^{-3} results in the presence of two zones with crossing of the diastereomer concentrations (Fig. 8b). In other words, the experimental data found in this work can account for a catalytic system moving from a zone of operating condition (PH_2) under which the concept lock-and-key would prevail to a zone where the major/minor concept would operate.

4. Conclusion

Two opposite effects of hydrogen pressure have been observed with the same catalytic complex Rh/(R,R)-Me-BPE for the hydrogenation of M-acrylate and E-emap. A kinetic study was undertaken to further understand this striking behaviour. Numerical integration using the entire concentration vs. time profiles provided values for the kinetic parameters of the Halpern type kinetic model. The substrates electronic properties influence the most enantioselective controlling steps, the oxidative addition of H_2 for E-emap and the coordination/decoordination step for M-acrylate, thereby explaining the opposed observed hydrogen pressure effects. To reach a more detailed understanding on the structure-ee and hydrogen pressure relationships, it seems advisable on the one hand to explore other catalytic systems as diverse as possible, and on the other hand to focus on steps (coordination and decoordination of substrate) upstream from oxidative addition and migratory insertion. Advances with the help of theoretical chemistry are on the way to help assigning the importance of these steps in the enantioselection process. It is also worth mentioning that this work represents one of the few experimental examples showing that the major/minor and the look-and-key principles can operate for the same catalytic system, the switch being driven by the hydrogen pressure.

Acknowledgements

The authors are grateful the Centre National de la Recherche Scientifique for financial support. A. ALOUI expresses special thanks for a PhD grant from the Région Rhône-Alpes through the special Cluster5-Chimie program.

Appendix A. Supplementary data

Supplementary data associated with this article can be found, in the online version, at http://dx.doi.org/10.1016/j.molcata.2012.06.012.

References

[1] R.A. Sheldon, Chiral Technologies, Marcel Dekker Inc., New York, 1993.
[2] A.N. Collins, G.N. Sheldrake, J. Grosby, Chirality in Industry, John Wiley and Sons, New York, 1992.
[3] I. Grayson, K. Drauz, Chim. Oggi 20 (2002) 15–19.
[4] E. Juaristi (Ed.), Enantioselective Synthesis of β-Amino Acids, Wiley-VCH, New York, 1997.
[5] D.C. Cole, Tetrahedron 50 (1994) 9517.
[6] M.T. Reetz, Angew. Chem. Int. Ed. 47 (2008) 2556–2588.
[7] C. Jaekel, R. Paciello, Chem. Rev. 106 (2006) 2912.
[8] N. Vriamont, B. Govaerts, P. Grenouillet, C. de Bellefon, O. Riant, Chem. Eur. J. 15 (2009) 6267–6278.
[9] R. Abdallaha, P. Grenouillet, N. Vriamont, O. Riant, C. De Bellefon, Comb. Chem. High Throughput Screen. 13 (2010) 393–413.
[10] A.S.C. Chan, J.J. Pluth, J. Halpern, J. Am. Chem. Soc. 102 (1980) 5952–5954.
[11] J. Halpern, Science 217 (1982) 401–407.
[12] J. Halpern, in: J.D. Morrison (Ed.), Asymmetric Synthesis, vol. 5, Academic Press, Orlando, 1985, pp. 41–69.
[13] C.R. Landis, J. Halpern, J. Am. Chem. Soc. 109 (1987) 1746–1754.
[14] B. McCulloch, J. Halpern, M.R. Thomas, C.R. Landis, Organometallics 9 (1990) 1392–1395.
[15] I. Ojima, T. Kogure, N. Yoda, J. Org. Chem. 45 (1980) 4728–4738.
[16] A. Marinetti, S. Jus, J.P. Genêt, Tetrahedron Lett. 40 (1999) 8365–8368.
[17] D. Heller, J. Holz, I.V. Komarov, H.J. Drexler, J. You, K. Drauz, A. Boener, Tetrahedron: Asymmetry 13 (2002) 2735–2741.
[18] Y. Sun, J. Wang, C. LeBlond, R.N. Landau, J. Laquirada, J.R. Sowa Jr., D.G. Blackmond, J. Mol. Catal. A 15 (1997) 495–502.
[19] J.M. Brown, P.A. Chaloner, J. Chem. Soc., Chem. Commun. (1980) 344–346.
[20] J.M. Brown, P.A. Chaloner, in: L.H. Pignolet (Ed.), Homogeneous Catalysis with Metal Phosphine Complexes, Plenum, New York, 1983, p. 137.
[21] L.H. Pignolet (Ed.), Plenum Press, NewYork, 1980, pp. 137–165.
[22] J.M. Brown, Chem. Soc. Rev. 22 (1993) 25–41.
[23] D.A. Evans, F.E. Michael, J.S. Tedrow, K.R. Campos, J. Am. Chem. Soc. 125 (2003) 3534–4354.
[24] T. Schmidt, W. Baumann, H.-J. Drexler, A. Arrieta, D. Heller, H. Buschmann, Organometallics 24 (2005) 3842–3848.
[25] H.-J. Drexler, W. Baumann, T. Schmidt, S. Zhang, A. Sun, A. Spannenberg, C. Fischer, H. Buschmann, D. Heller, Angew. Chem. 117 (2005) 1208–1212.
[26] T. Schmidt, Z. Dai, H.-J. Drexler, W. Baumann, C. Jäger, D. Pfeifer, D. Heller, Chem. Eur. J. 14 (2008) 4469–4471.
[27] K.V.L. Crépy, T. Imamoto, Adv. Synth. Catal. 345 (2003) 79–101.
[28] J.M. Brown, R. Giernoth, Curr. Opin. Drug Discov. Dev. 3 (2000) 825.
[29] I.D. Gridnev, T. Imamoto, Acc. Chem. Res. 37 (2004) 633.
[30] I.D. Gridnev, N. Higashi, K. Asakura, T. Imamoto, J. Am. Chem. Soc. 122 (2000) 7183–7194.
[31] I.D. Gridnev, Y. Yamanoi, N. Higashi, H.H. Tsuruta, M. Yasutake, T. Imamoto, Adv. Synth. Catal. 343 (2001) 118–136.
[32] M. Alame, N. Pestre, C. De Bellefon, Adv. Synth. Catal. 350 (2008) 898–908.
[33] P.J. Donoghue, P. Helquist, O. Wiest, J. Org. Chem. 72 (2007) 839–847.
[34] B.D. Vineyard, W.S. Knowles, M.J. Sabacky, G.L. Bachman, D.J. Weinkauff, J. Am. Chem. Soc. 99 (1977) 5946–5952.
[35] S.-G. Lee, Y.J. Zhang, Org. Lett. 4 (2002) 2429–2431.

[36] Q. Liu, F. Takemura, A. Yabe, J. Chem. Eng. Data 41 (1996) 1141–1143.
[37] K. Radhakrishnan, P.A. Ramachandran, P.H. Brahme, R.V. Chaudhari, J. Chem. Eng. Data 28 (1983) 1–4.
[38] W. Tang, X. Zhang, Angew. Chem. Int. Ed. 41 (2002) 1612–1614.
[39] React'Op was developed by Russian Scientific Center of Applied Chemistry and ChemInform-St.Petersburg Ltd.
[40] S. Feldgus, C.R. Landis, J. Am. Chem. Soc. 122 (2000) 12714–12727.
[41] Rate constant are given in supplementary information.
[42] M. Yasutake, I.D. Gridnev, N. Higashi, T. Imamoto, Org. Lett. 3 (2001) 1701–1704.
[43] S. Feldgus, C.R. Landis, Organometallics 20 (2001) 2374–2386.
[44] T. Schmidt, Z. Dai, H.-J. Drexler, M. Hapke, A. Preetz, D. Heller, Chem. Asian. J. 3 (2008) 1170–1180.